Structures, solvatochromism, protonation and photoswitching of tetra-(*ortho*)-substituted azobenzenes bearing 3,5-dimethoxy groups

Sandra Ramírez-Rave, Marcos Flores Alamo and Anatoly K. Yatsimirsky
Facultad de Química, Universidad Nacional Autónoma de México, 04510 CDMX, México

Electronic supplementary information

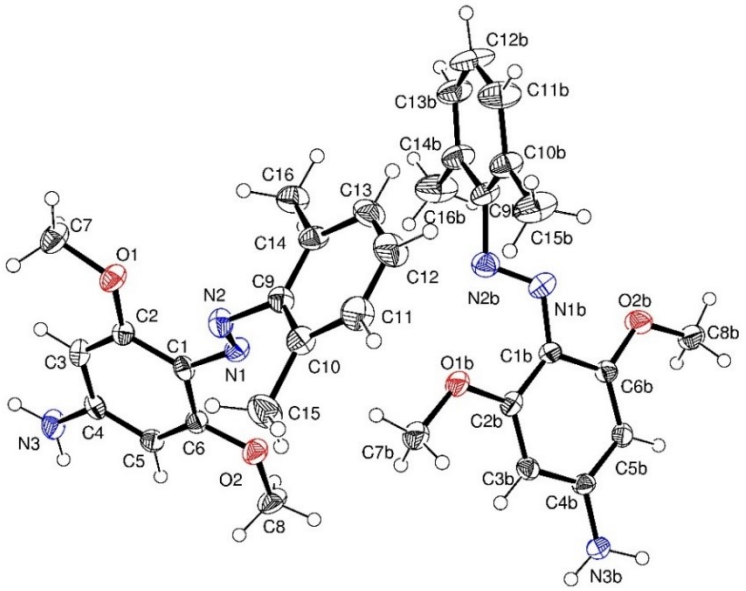

Fig. S1. ORTEP drawing of the structure of compound **1**. Non-H atoms are represented by 50% probability ellipsoids and H atoms are shown as small circles of an arbitrary size.

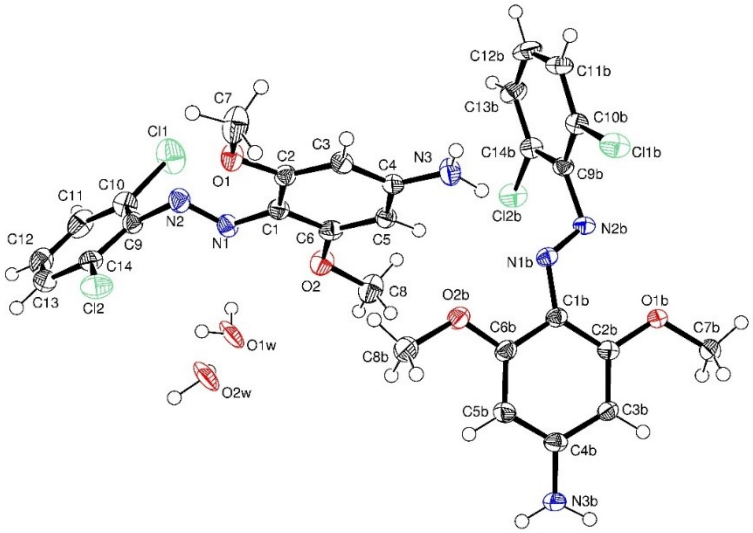

Fig. S2. ORTEP drawing of the structure of compound **2**. Non-H atoms are represented by 50% probability ellipsoids and H atoms are shown as small circles of an arbitrary size. The atoms O1w and O2w are disordered over two sites with occupancies 0.50:0.50.

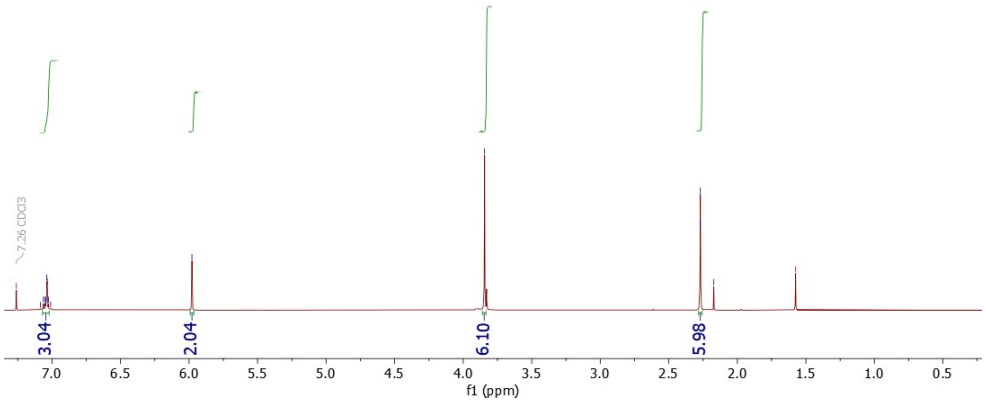

Fig. S3. ^{1}H NMR spectrum of **1** in $CDCl_3$.

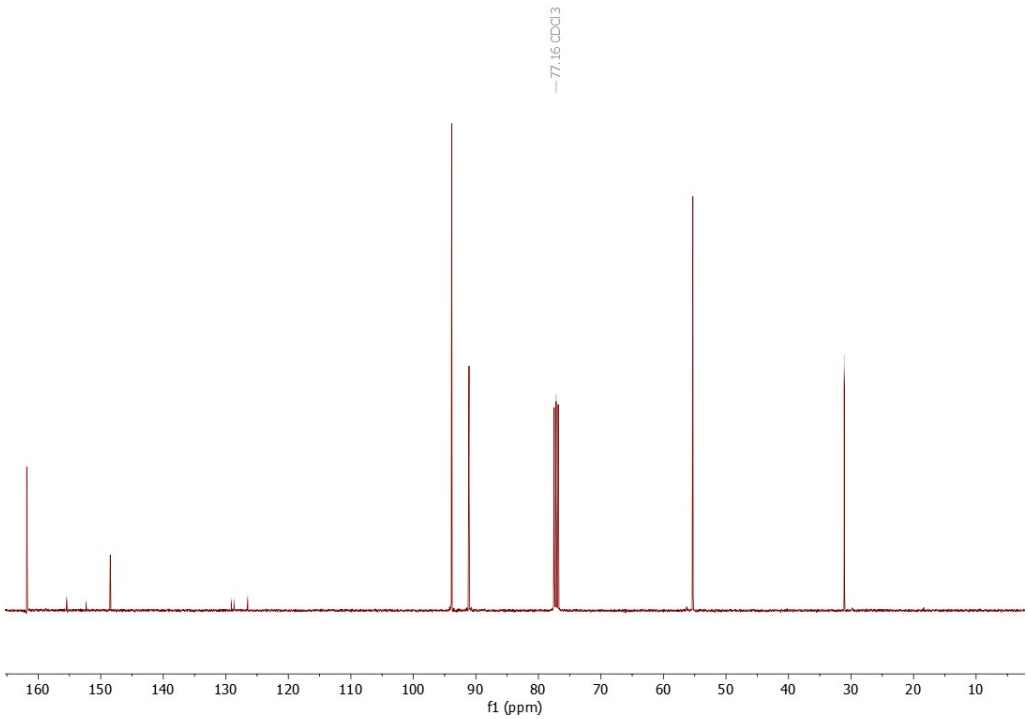

Fig. S4. ^{13}C NMR spectrum of **1** in $CDCl_3$.

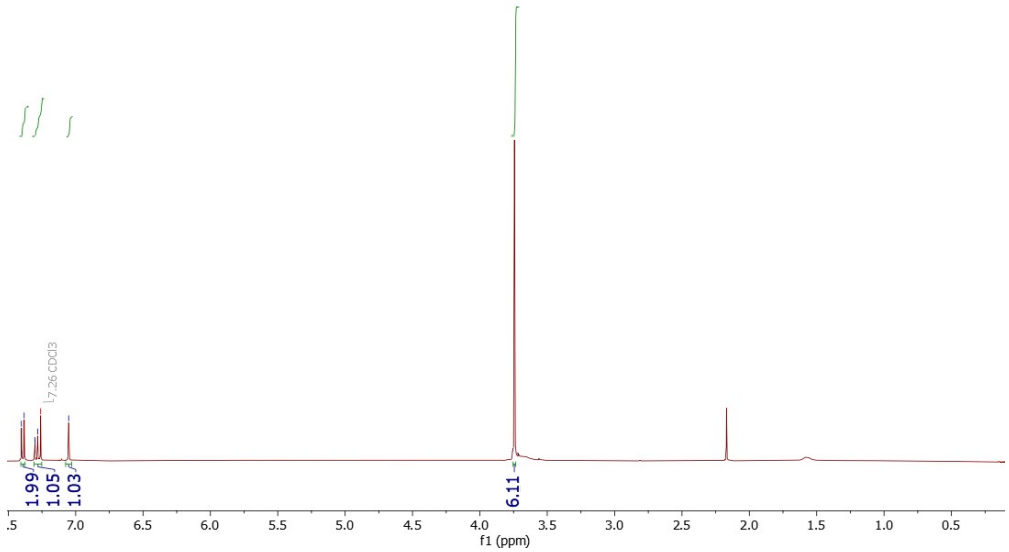

Fig. S5. ^{1}H NMR spectrum of **2** in $CDCl_3$.

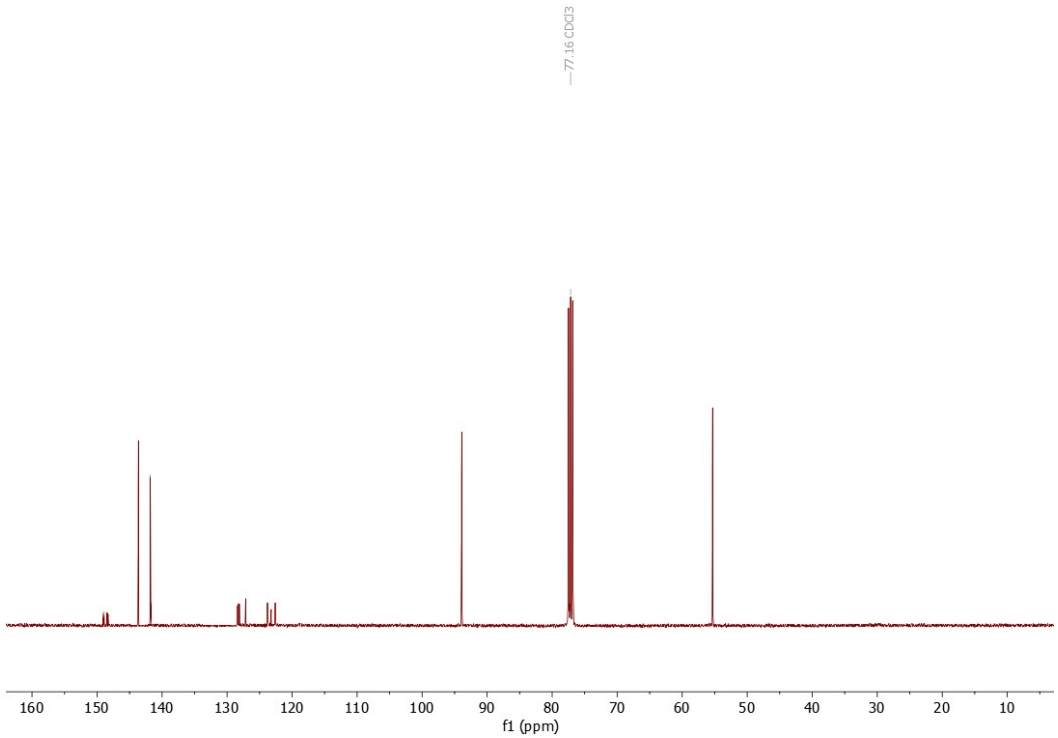

Fig. S6. ^{13}C NMR spectrum of **2** in $CDCl_3$.

Table S1. Statistical data for multiparameter linear fit of the results of Table 2 to equations (1) – (3).

Comp.	Eq.	Band	Coefficient	Value	Standard Error	t-Value	Prob>|t|
1	(1)	$\tilde{\nu}_{max1}$	s	-307.03	145.18	-2.11	0.05433
			a	-39.73	99.70	-0.40	0.69673
			b	-1378.54	142.08	-9.70	2.55075E-7
2	(1)	$\tilde{\nu}_{max1}$	s	-775.55	110.11	-7.04341	8.75601E-6
			a	-461.53	75.62	-6.10349	3.75914E-5
			b	-1373.89	107.76	-12.74981	1.00681E-8
1	(1)	$\tilde{\nu}_{max2}$	s	154.95	110.70	1.39971	0.18501
			a	993.67	76.02	13.07052	7.45016E-9
			b	-282.30	108.34	-2.60572	0.02177
2	(1)	$\tilde{\nu}_{max2}$	s	-929.59	257.58	-3.60898	0.00318
			a	180.66	176.89	1.02136	0.32571
			b	-759.89	252.07	-3.01458	0.00996
1	(2)	$\tilde{\nu}_{max1}$	s	-1296.51	738.88	-1.7547	0.10478
			d	-185.97	230.00	-0.80855	0.43451
			a	-522.55	212.38	-2.46049	0.03001
			b	-1517.84	224.14	-6.77197	1.98063E-5
2	(2)	$\tilde{\nu}_{max1}$	s	-1634.22	552.19	-2.9595	0.01193
			d	-625.32	171.89	-3.63792	0.0034
			a	-1030.18	158.72	-6.49065	2.97704E-5
			b	-1497.39	167.51	-8.93931	1.18581E-6

1	(2)	$_{max2}$	s	-1194.61	768.84	-1.55377	0.1462
			d	272.98	239.33	1.1406	0.27629
			a	1070.41	220.99	4.84373	4.02496E-4
			b	-144.50	233.23	-0.61955	0.54714
2	(2)	$_{max2}$	s	-1716.74	1221.31	-1.40565	0.18519
			d	-683.02	380.18	-1.7966	0.0976
			a	-38.36	351.04	-0.10928	0.91479
			b	-682.75	370.48	-1.84288	0.09018
1	(3)	$_{max1}$	di	-1025.23	748.26	-1.37016	0.19573
			e	-184.15	228.73	-0.8051	0.43642
			a	-199.88	136.61	-1.46311	0.16913
			b	-1593.71	238.92	-6.67051	2.29143E-5
2	(3)	$_{max1}$	di	-1580.47	538.99	-2.93228	0.01255
			e	-739.59	164.76	-4.4889	7.40836E-4
			a	-529.44	98.41	-5.38014	1.65318E-4
			b	-1379.67	172.10	-8.01666	3.68066E-6
1	(3)	$_{max2}$	di	-291.15	644.97	-0.45143	0.65973
			e	282.45	197.15	1.43265	0.17749
			a	780.29	117.75	6.62635	2.44257E-5
			b	-398.43	205.94	-1.9347	0.07695
2	(3)	$_{max2}$	di	-1454.39	1373.31	-1.05903	0.31044
			e	-397.69	419.80	-0.94734	0.36215
			a	-26.41	250.73	-0.10535	0.91784
			b	-1030.84	438.50	-2.35083	0.03666

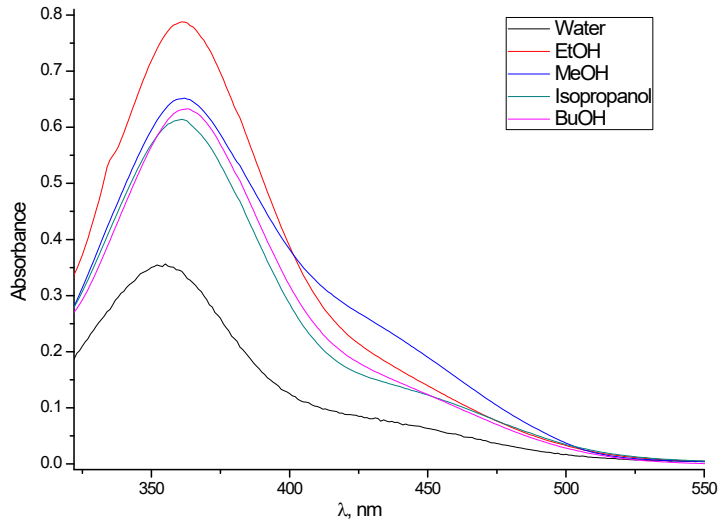

Fig. S7. UV-Vis spectra of **1** in neutral form (polar protic solvents).

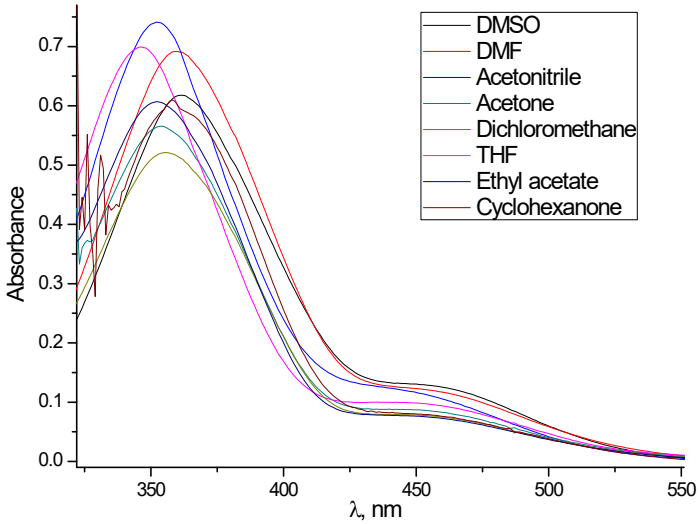

Fig. S8. UV-Vis spectra of **1** in neutral form (polar non-protic solvents).

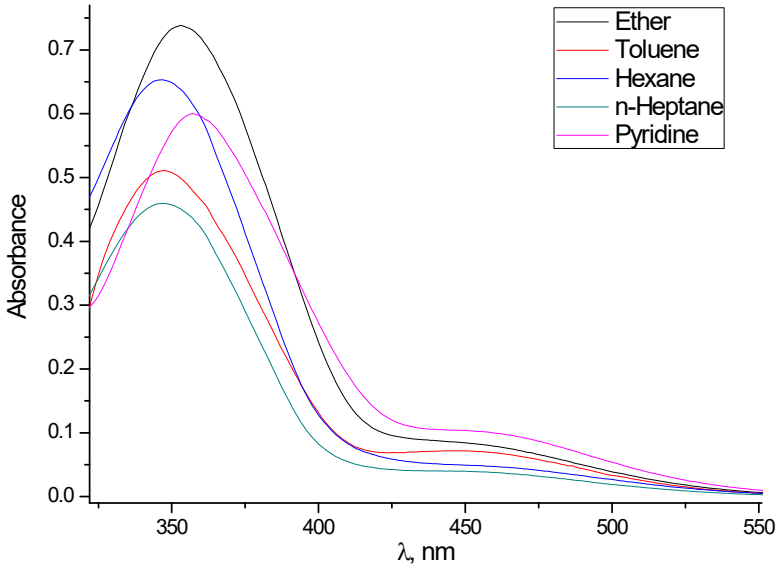

Fig. S9. UV-Vis spectra of **1** in neutral form (non-polar solvents).

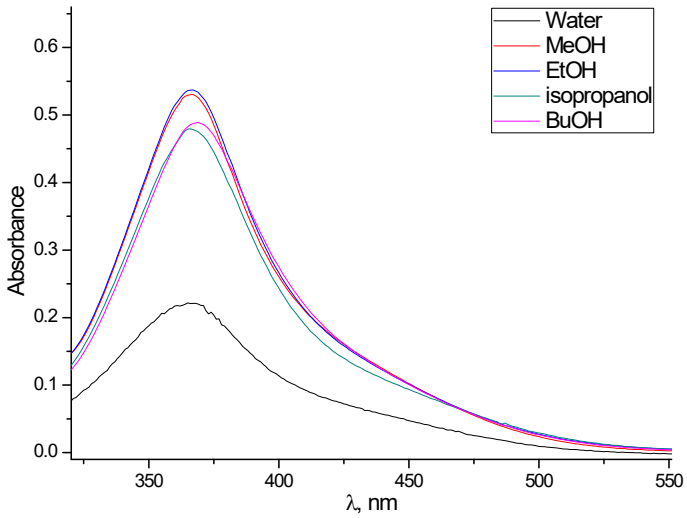

Fig. S10. UV-Vis spectra of **2** in neutral form (polar protic solvents).

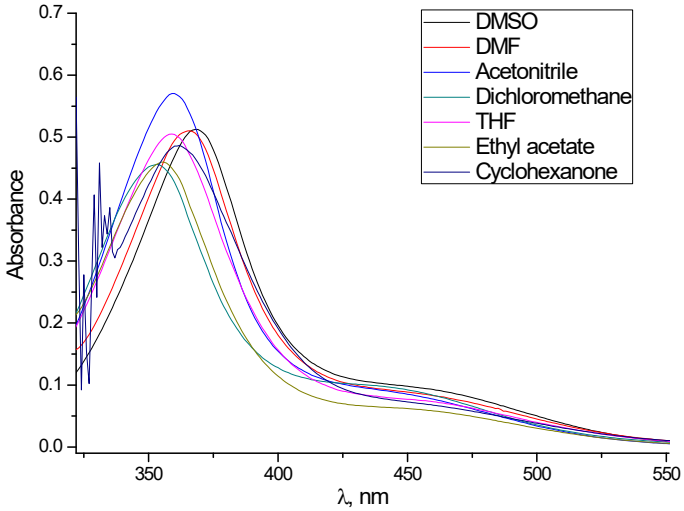

Fig. S11. UV-Vis spectra of **2** in neutral form (polar non-protic solvents).

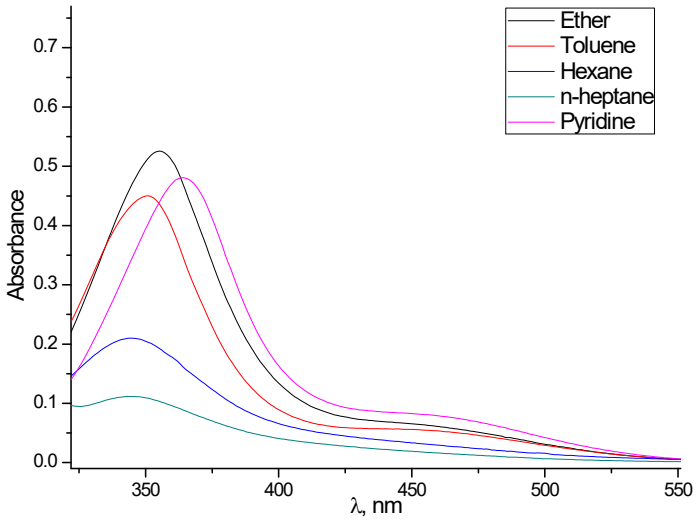

Fig. S12. UV-Vis spectra of **2** in neutral form (non-polar solvents).

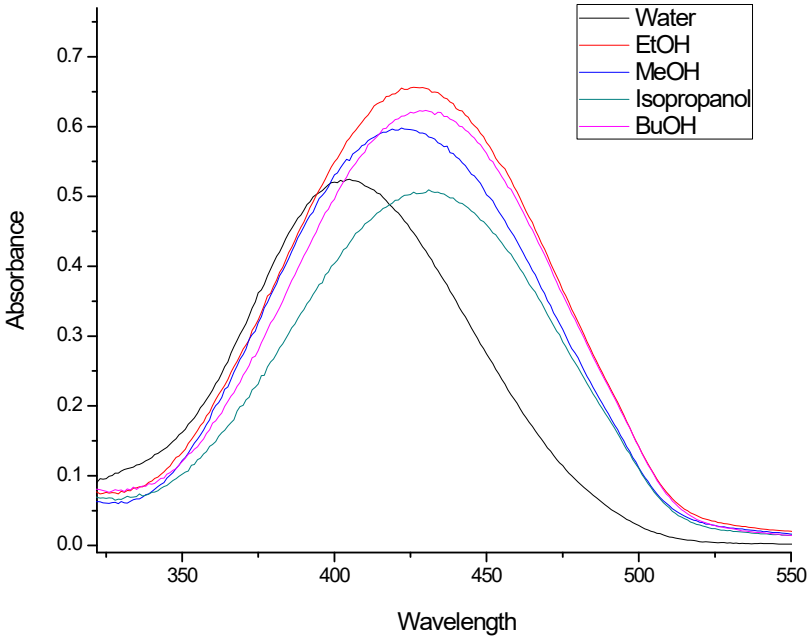

Fig. S13. UV-Vis spectra of **1** in protonated form (polar protic solvents).

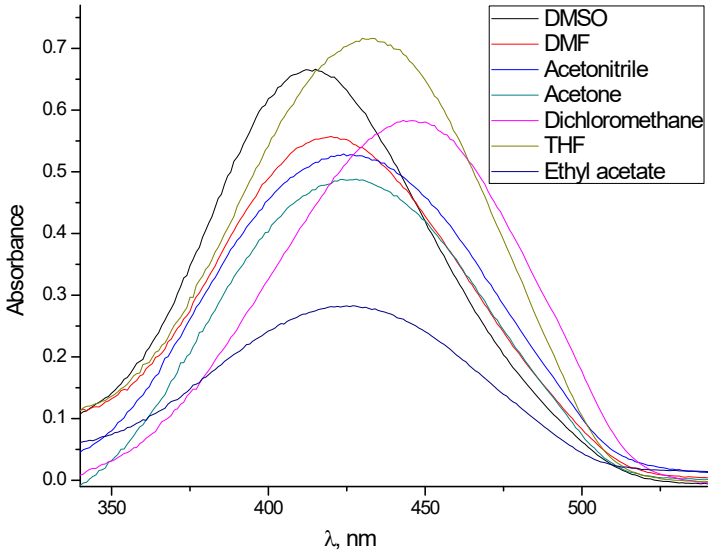

Fig. S14. UV-Vis spectra of **1** in protonated form (polar non-protic solvents).

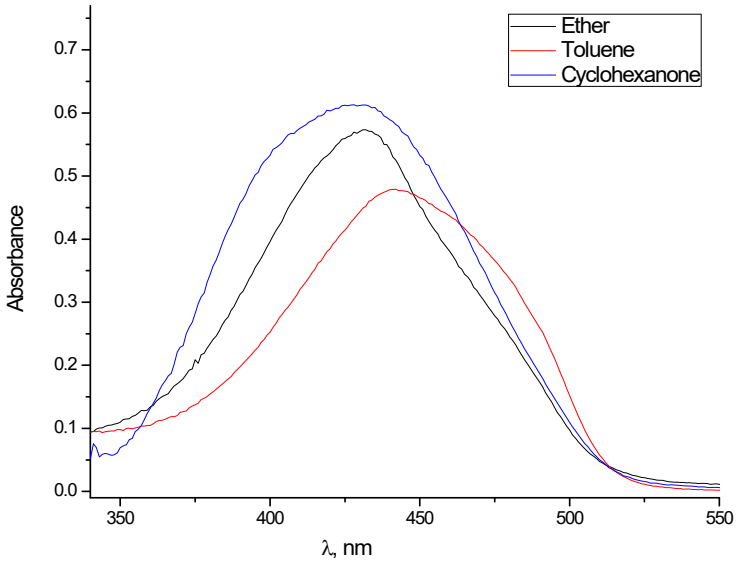

Fig. S15. UV-Vis spectra of **1** in protonated form (non- polar solvents).

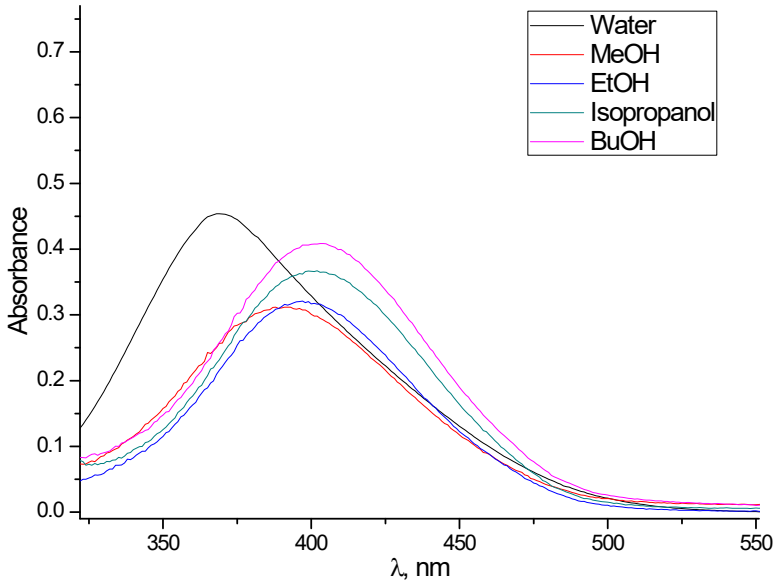

Fig. S16. UV-Vis spectra of **2** in protonated form (polar protic solvents).

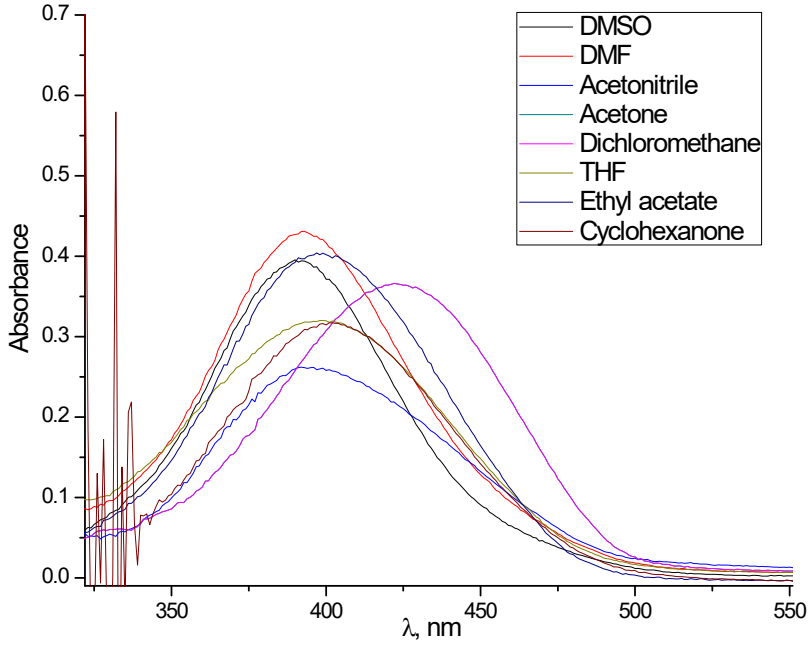

Fig. S17. UV-Vis spectra of **2** in protonated form (polar non-protic solvents).

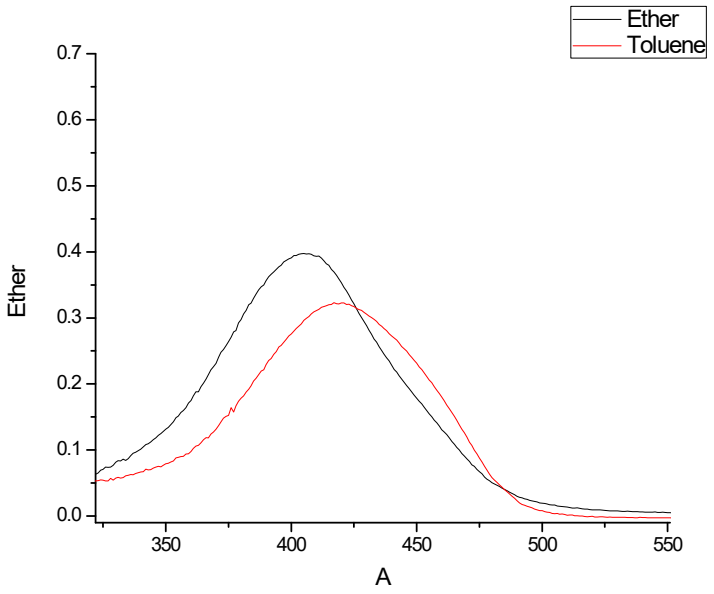

Fig. S18. UV-Vis spectra of **2** in protonated form (non- polar solvents).

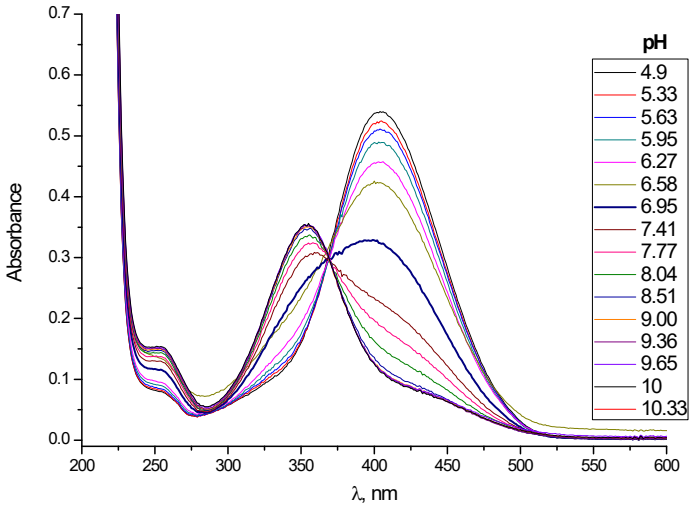

Fig. S19. Spectrophotometric pH-titration of **1** in H_2O in a 0.02 M mixture of MES, MOPS and CHES buffers.

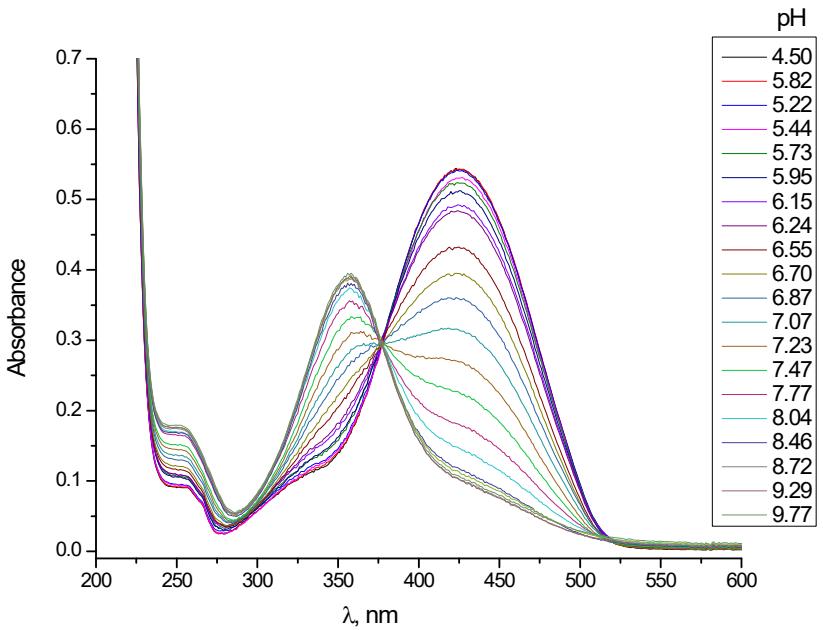

S20. Spectrophotometric pH-titration of **1** in H_2O-EtOH 50/50 v/v in a 0.02 M mixture of MES, MOPS and CHES buffers

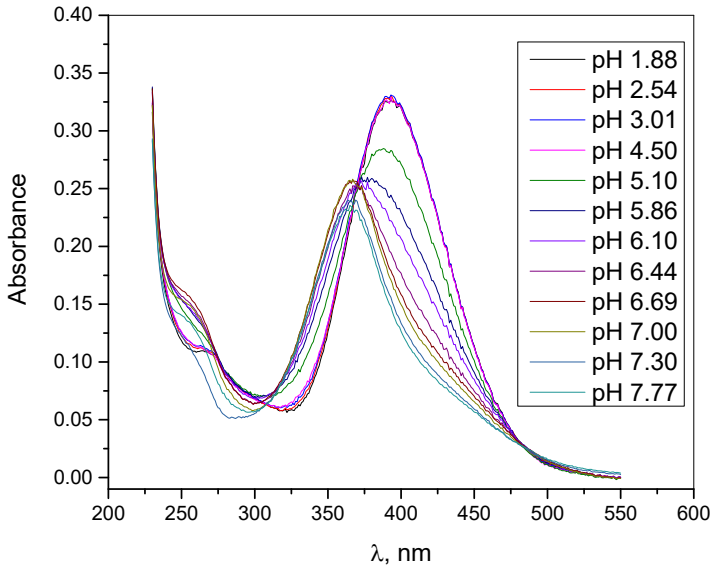

Fig. S21. Spectrophotometric pH-titration of **2** in H_2O in a 0.02 M mixture of MES, MOPS and CHES buffers.

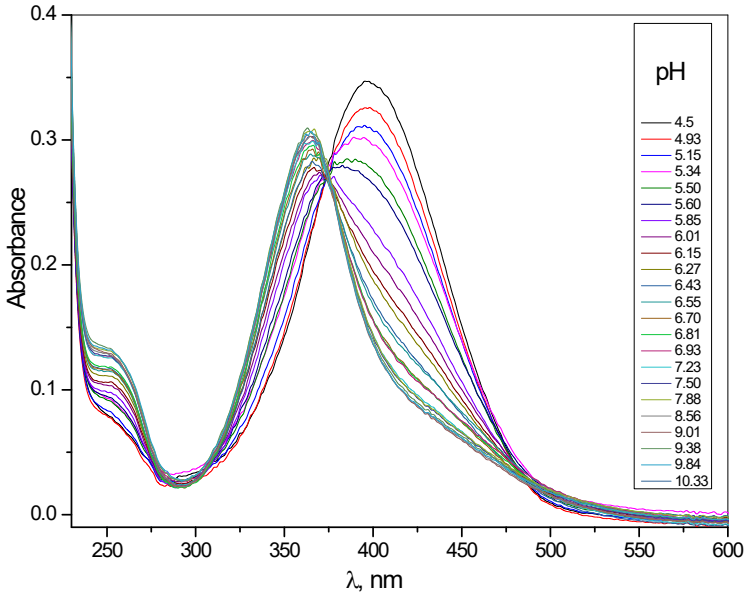

Fig. S22. Spectrophotometric pH-titration of **2** in H_2O-EtOH 50/50 v/v in a 0.02 M mixture of MES, MOPS and CHES buffers

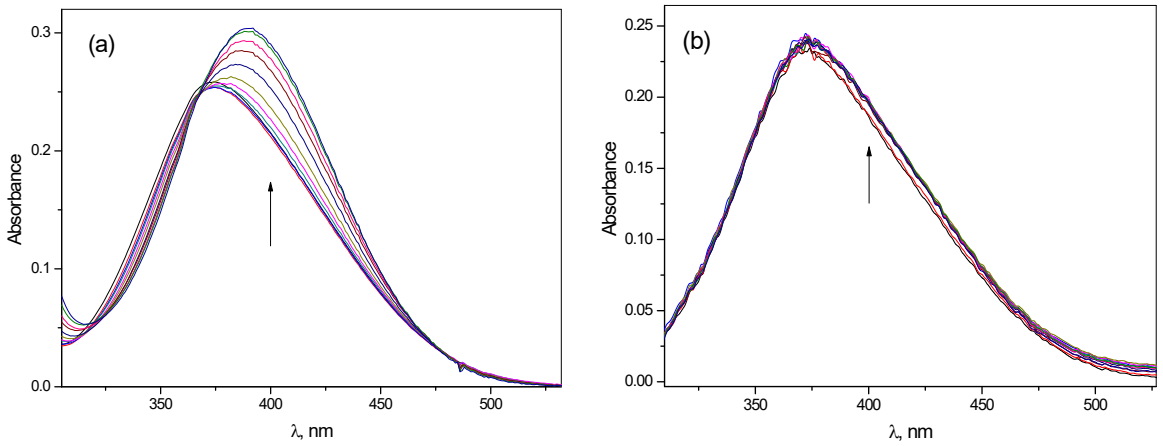

Fig. S23. Spectrophotometric titration of 25 mM **2** by 0 – 1 mM CuSO4 (a) and 0 – 5 mM ZnSO4 (b) at pH 6. Arrows show the direction of spectral changes induced by increased concentrations of the metal ion.

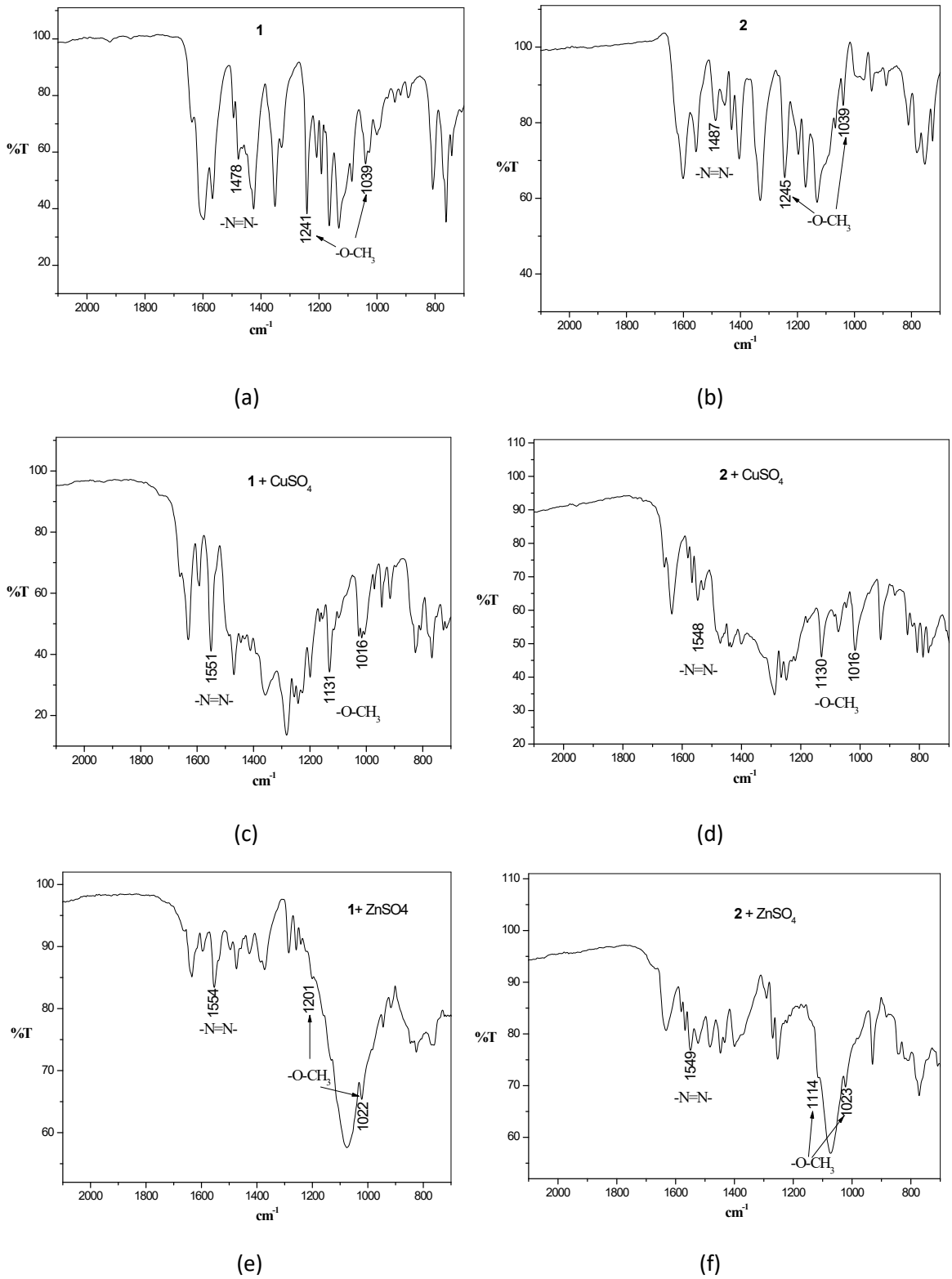

Fig. S24. FTIR spectra of free **1** (a) and **2** (b) and their complexes with Cu(II), (c) and (d): and Zn(II), (e) and (f), as solid powders. Metal complexes were prepared by mixing a

neutral ligand, **1** or **2**, with metal sulfate in methanol in the 1:1 molar ratio. Precipitated complexes were dried to remove rests of the solvent.

The characteristic bands of azo and methoxy groups were assigned considering established ranges of their absorption (P. Larkin, Infrared and Raman Spectroscopy: Principles and Spectral Interpretation, 2011, Elsevier) and reported results for other azobenezene derivatives (G.-Y. Yeap et al., *J. Mol. Struct*. 2008, **882**, 1–8; D. R. Armstrong, J. Clarkson, and W. E. Smith, *J. Phys. Chem*. 1995, **99**, 17825-17831; H. F. Babamale et al., *J. Mol. Struct*. 2021, **1232**, 130049).

The complexation with Cu(II) and Zn(II) shifts the band of the azo group to higher frequencies, which is unusual. However, similar shifts were recently reported for Cu(II) complexes of some *ortho*-hydroxy and *ortho*-amino azobenzenes (J. L. Pratihar et al., *Polyhedron*, 2019, **161**, 317–324; S. M. Emama, et al., *Int. J. Eng. Res. & Tech.*, 2017, **6**, 354-364) and probably are common for ortho-substituted azobenzenes in general.

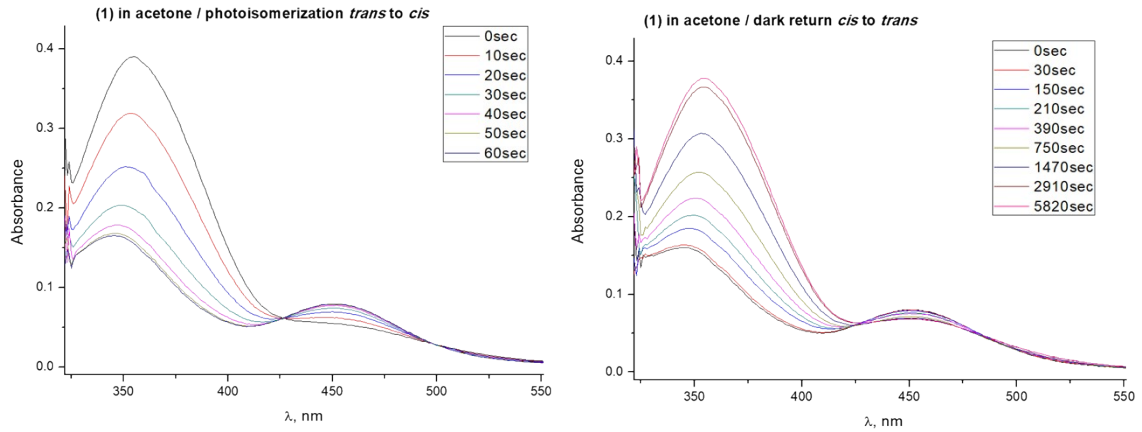

Fig. S25. UV-Vis spectra of photoisomerization of **1** in acetone at 360 nm.

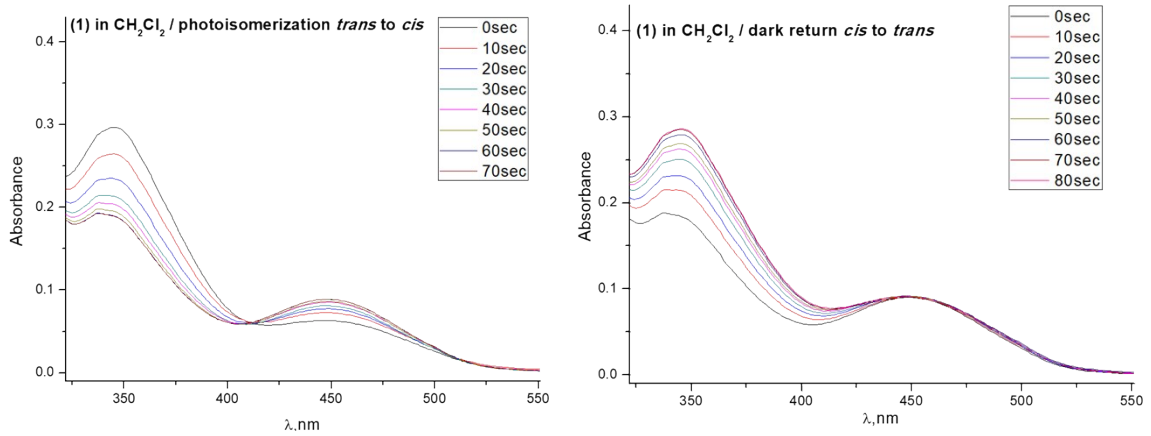

Fig. S26. UV-Vis spectra of photoisomerization of **1** in dichloromehane at 360 nm.

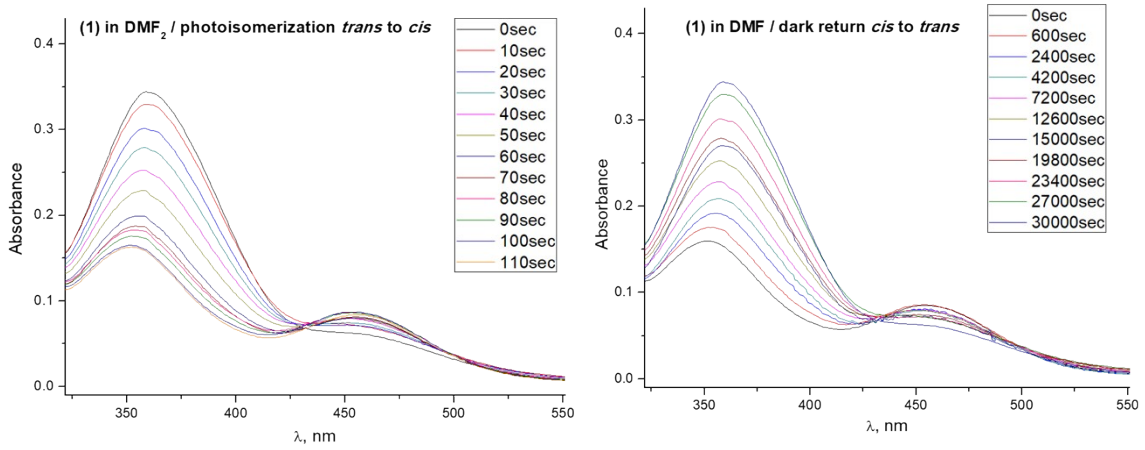

Fig. S27. UV-Vis spectra of photoisomerization of **1** in dimethylformamide at 360 nm.

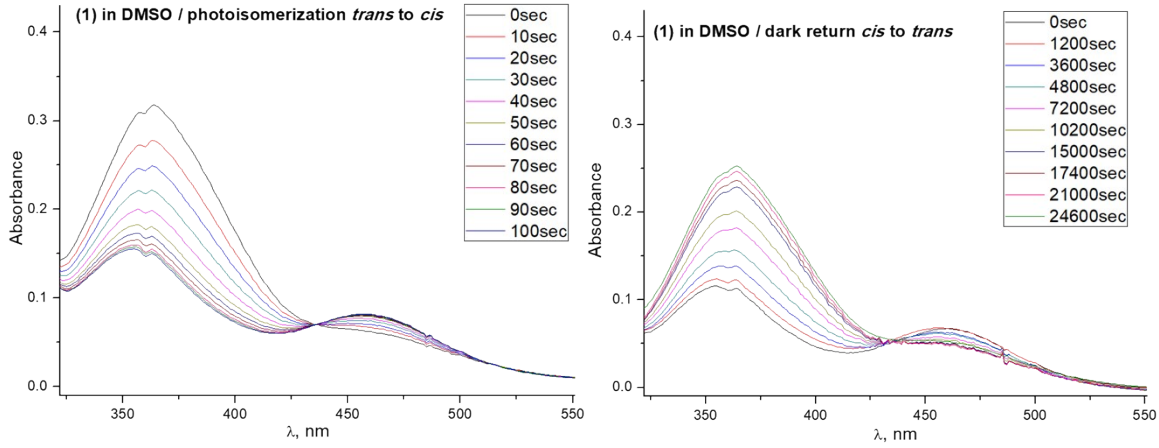

Fig. S28 UV-Vis spectra of photoisomerization of **1** in dimethyl sulfoxide at 360 nm.

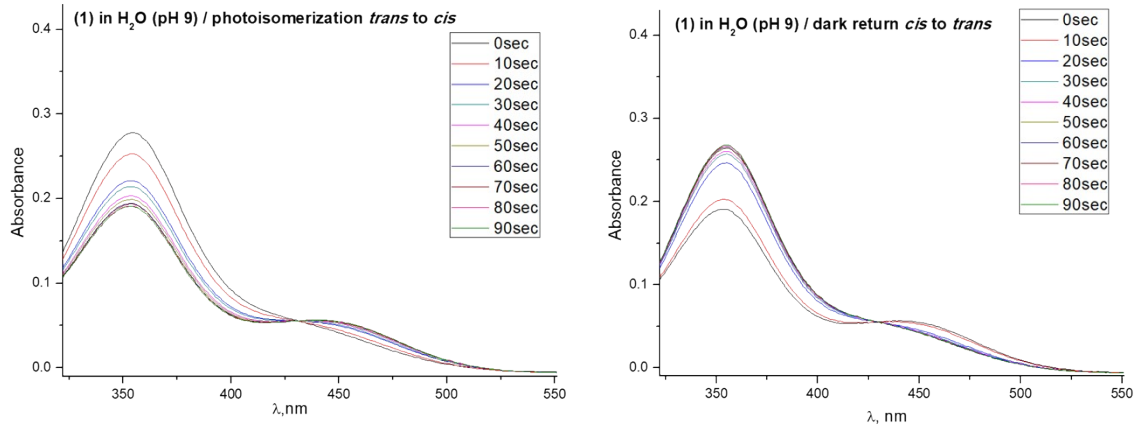

Fig. S29. UV-Vis spectra of photoisomerization of **1** in H_2O (pH 9) at 360 nm.

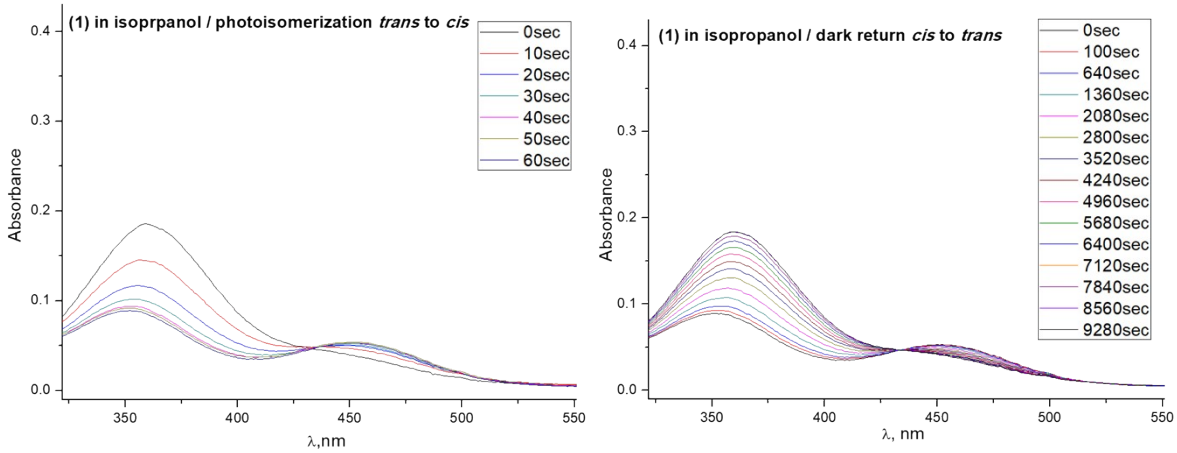

Fig. S30. UV-Vis spectra of photoisomerization of **1** in isopropanol at 360 nm.

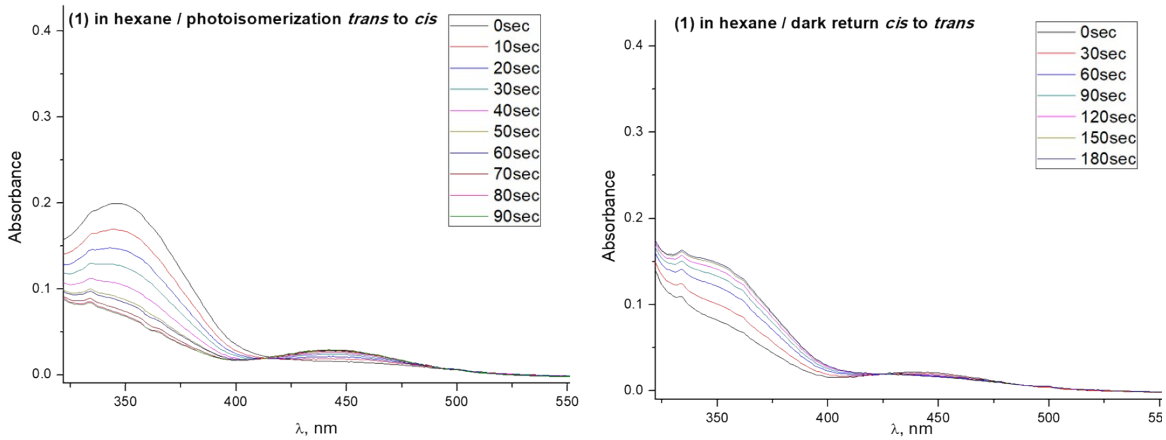

Fig. S31. UV-Vis spectra of photoisomerization of **1** in hexane at 360 nm.

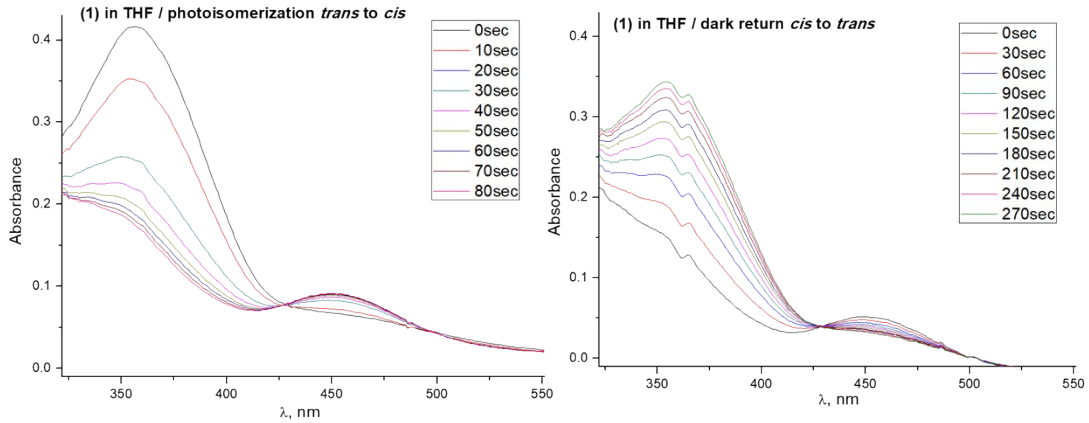

Fig. S32. UV-Vis spectra of photoisomerization of **1** in tetrahydrofuran at 360 nm.

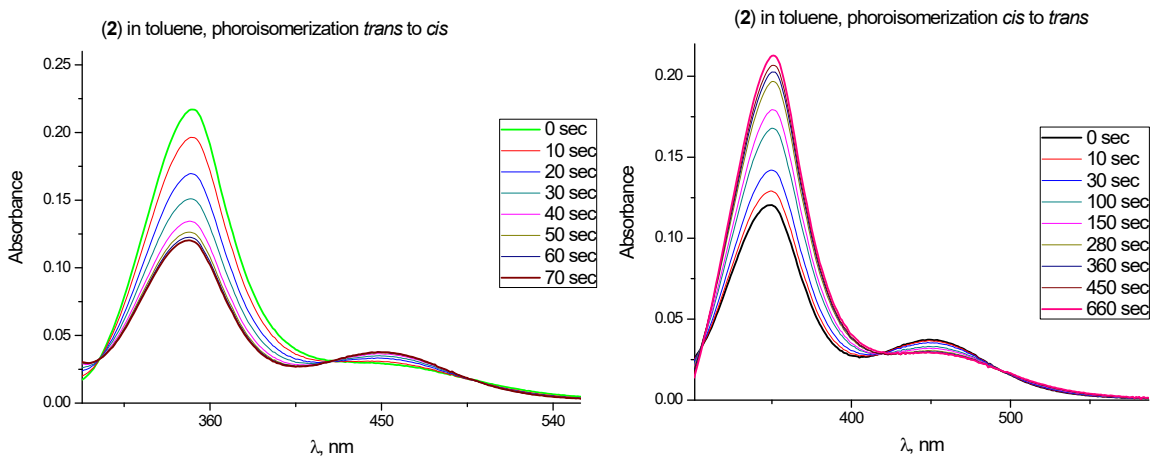

Fig. S33. UV-Vis spectra of photoisomerization of **2** in toluene at 360 nm.

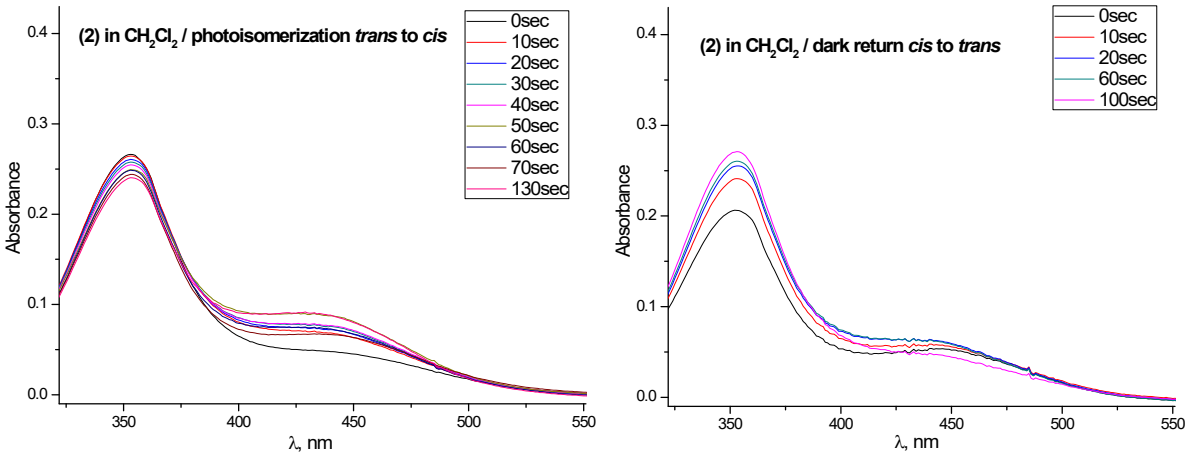

Fig. S34. UV-Vis spectra of photoisomerization of **2** in dichloromethane at 360 nm.

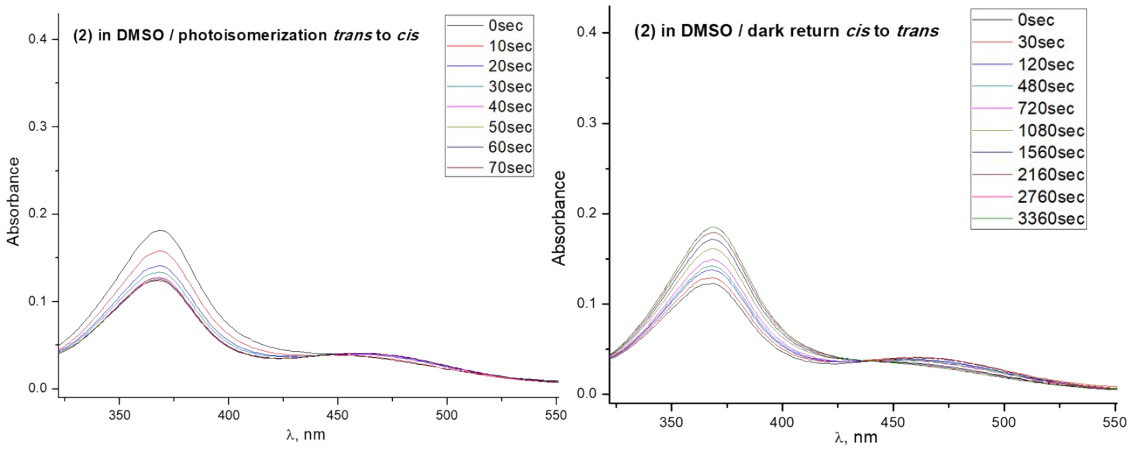

Fig. S35. UV-Vis spectra of photoisomerization of **2** in dimethyl sulfoxide at 360 nm.

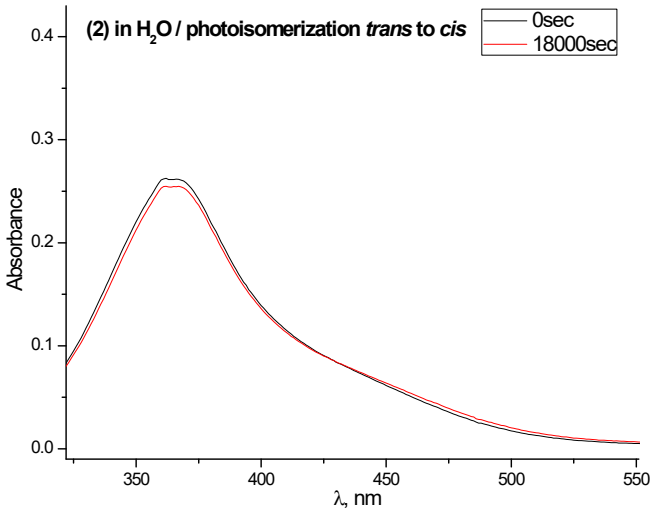

Fig. S36. UV-Vis spectra of photoisomerization of **2** in H_2O (pH 9) at 360 nm.

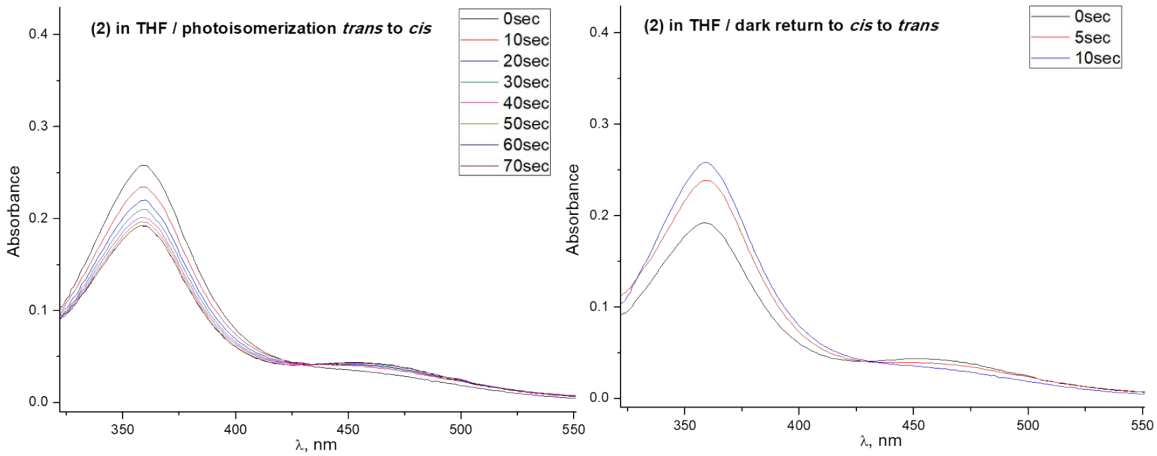

Fig. S37. UV-Vis spectra of photoisomerization of **2** in THF at 360 nm.